

## Abstract

Seismic signals are considerably amplified by earth neutral atmosphere and then revealed to remote sensing by their interaction with the ionosphere. Such acoustic-gravity waves are detectable punctually after high magnitude earthquakes since the 1960s. Most recently, Total Electronic Content (TEC) extracted from GPS data gave the way to a global visualization of the horizontal propagation of ionospheric seismic waves. These are excited through a coupling mechanism between the neutral atmosphere and the ionosphere that will be detailed here. Therefore the general equations of the magneto-hydrodynamics are reminded and the key ionospheric parameters quantified, preliminary to any approximation by the use of classical ionospheric models.

From now on, after imaging seismic waves in the ionosphere, challenging is the characterization of the seismic source, where coupling mechanisms between the solid earth and its atmosphere are involved. The study here is based on the TEC variations observed close to the source shortly after the earthquake that occurred in the Tokachi-Oki region (Japan) in 2003, September the 25th, by referring to the displacement mechanism described by [Yagi, Y., 2004]. A modelling of the horizontal and vertical propagation of acoustic waves generated by three distinct sources distributed along a single fault are developed, and the preliminary results of the GPS data inversion tests are presented in this work.

### Earth – Neutral Atmosphere – Ionosphere Coupling

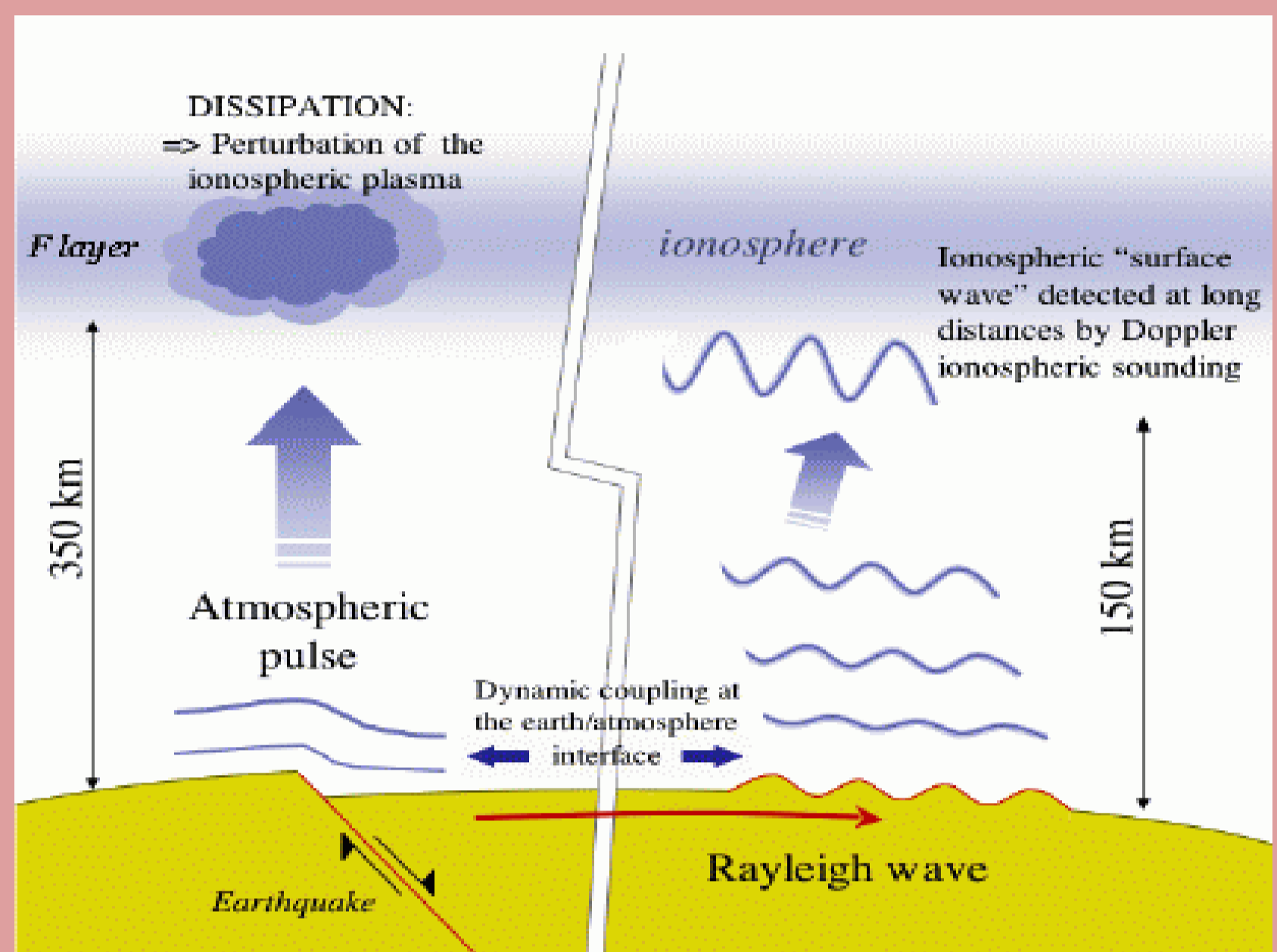


Fig.1 : Coupling mechanisms involved consecutively to an earthquake.

Vertical ground displacements generate atmospheric pressure waves. Those are considerably amplified upward to the ionosphere under the effect of the decreasing density.

The ionospheric waves at **near field** (< 1000 km) originate directly from the earthquake rupture process and at teleseismic distance the perturbations are the consequence of Rayleigh surface waves.

### Tokachi-Oki Earthquake : GPS ionospheric seismic wave imaging

The earthquake (Mw 8,3) occurred at 19:50 UT and induced strong vertical ground motion. The epicenter was located at 144,1°W-42,2°N (red cross, see on fig.2).

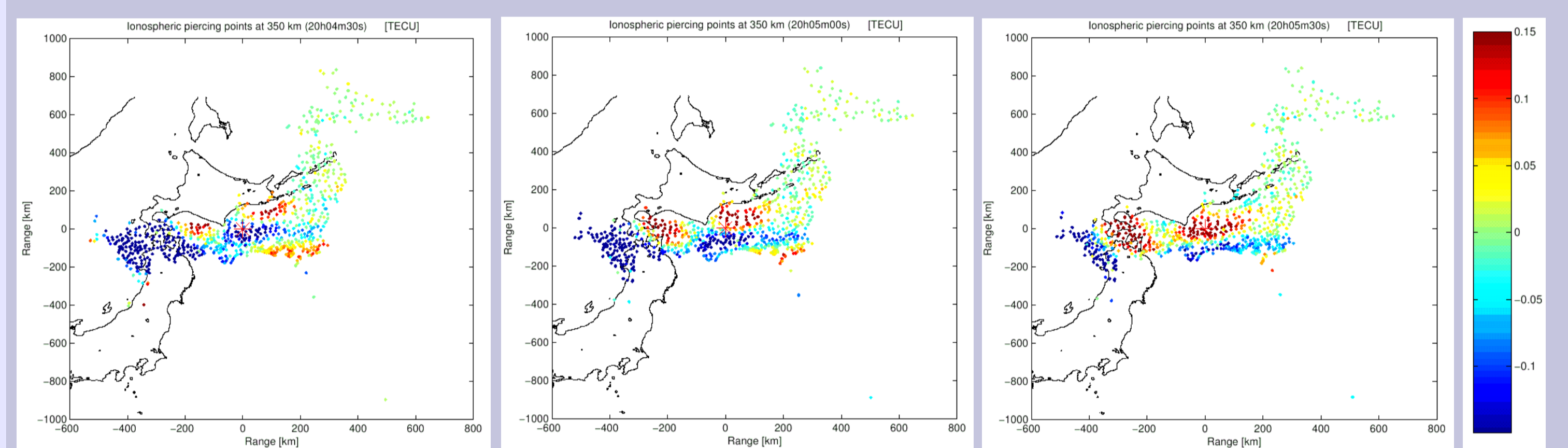


Fig. 2 : Time sequence of STEC at ionospheric piercing points for satellite PRN13. From TEC extraction tool by [Crespon, F., 2007].

### Near source modelling

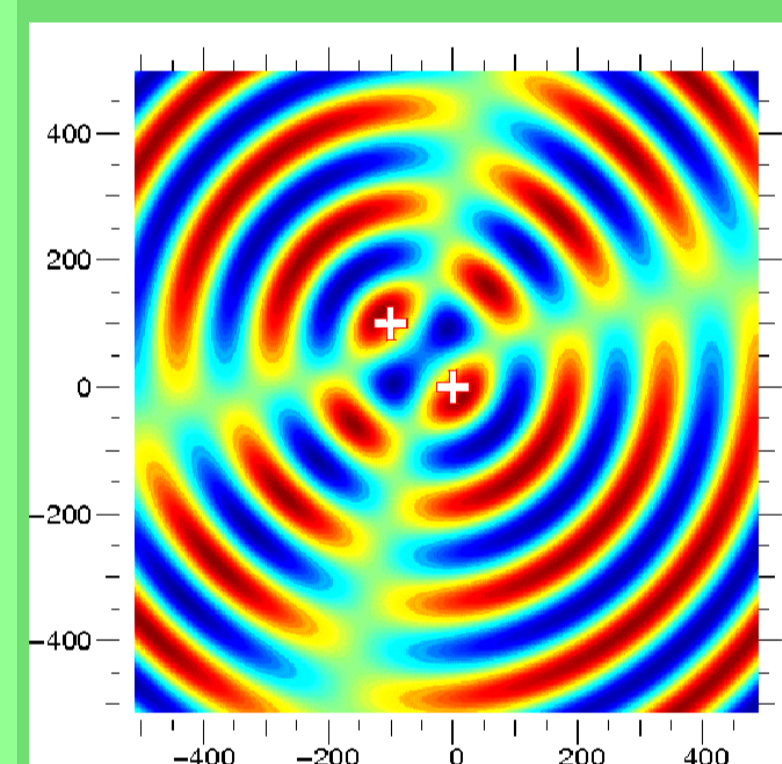


Fig. 3 : Synthetic of two acoustic sources that radiate coherently.

#### Direct problem

Phase inversions observed at TEC images (see fig.2) are interpreted here as interferences between separated sources, as shown by fig.3. [Yagi, Y., 2004] corroborates this assumption : he identified 3 centers of coseismic displacements along a single fault. So we modelled each of them as an acoustic source :

The inversion procedure is posed as a least-square problem. Wavelengths exceeding 300 km are found as shown fig.4, so other parameters have to be taken into account. Ingredients for the integration of the perturbed electronic density along the line of sight are based on the determination of the neutral density variations by ray tracing, linked to the electronic density variation. Both steps are illustrated by fig. 5 and fig.6 below.

#### Ray tracing

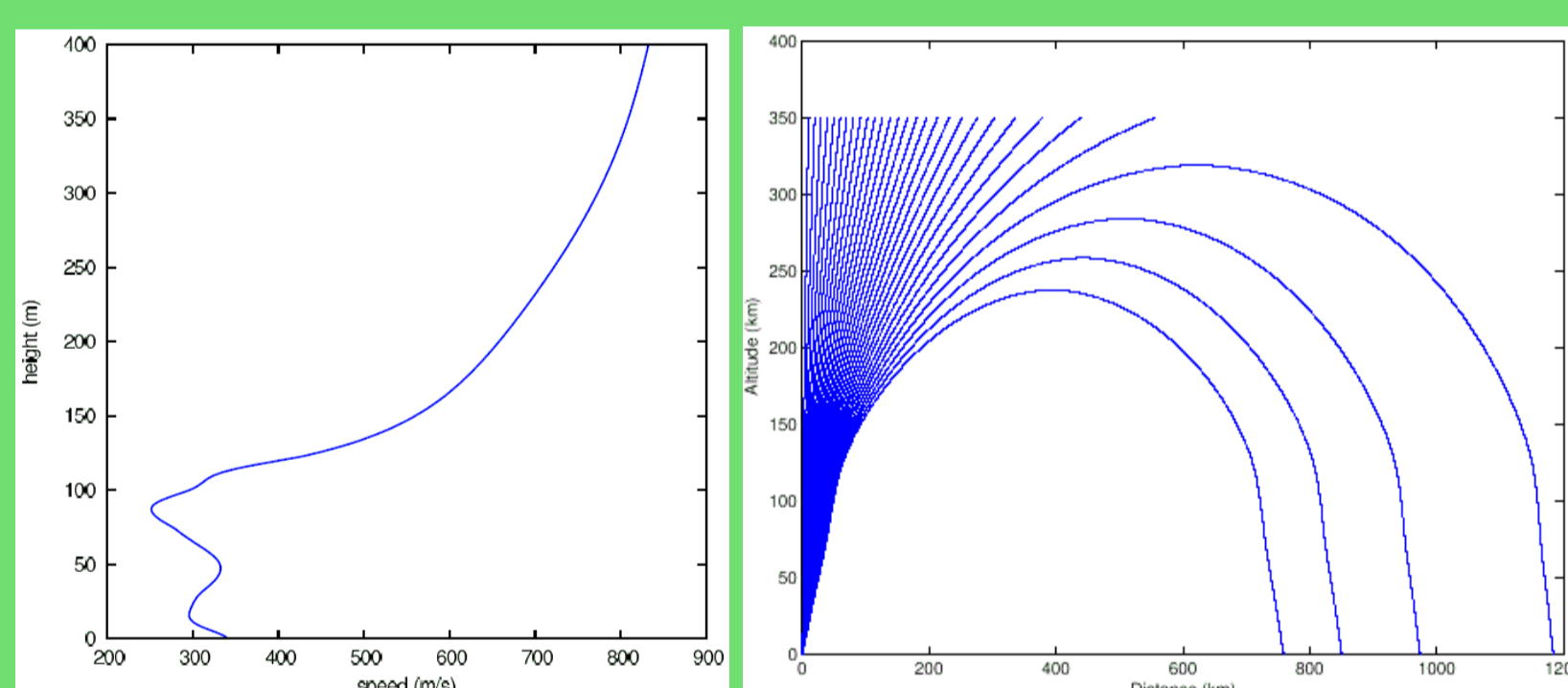


Fig.5 Due to the speed of sound variations (right) trajectories of rays are deflected (left, represented for varying initial incident angles).

#### Neutral atmosphere and plasma coupling

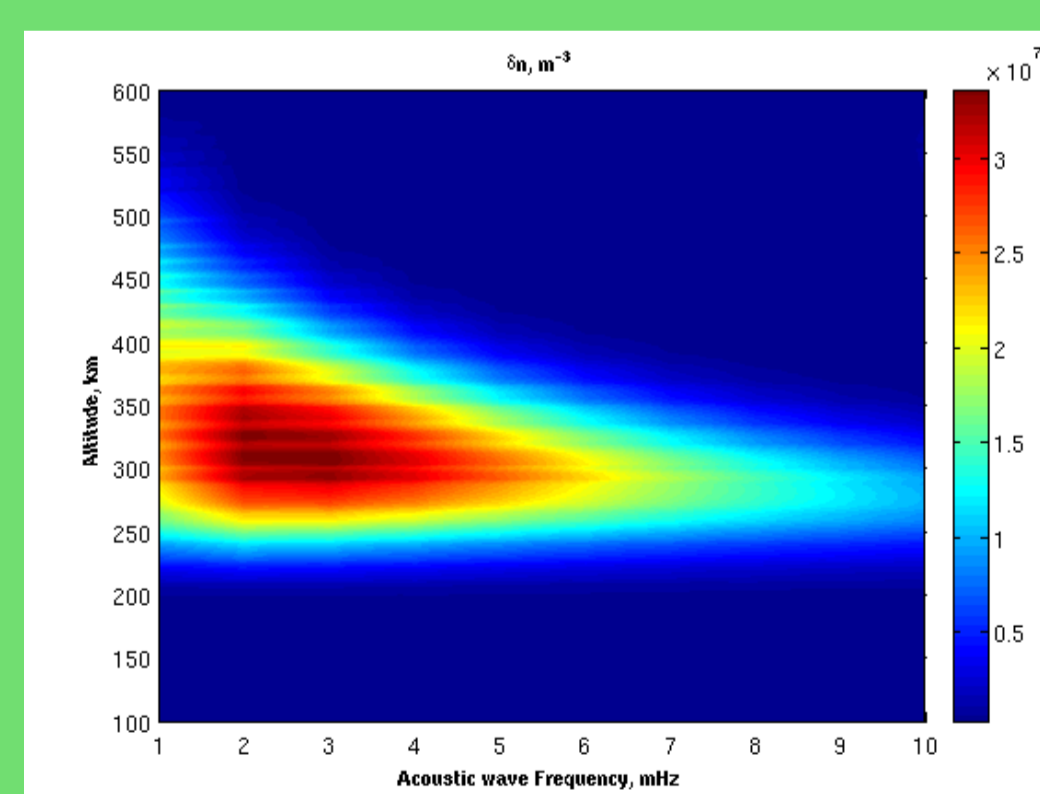


Fig.6 Conversion relation and frequency dependence between incident acoustic wave (from neutral atmosphere) and the resulting electronic density variation.

### Inversion process

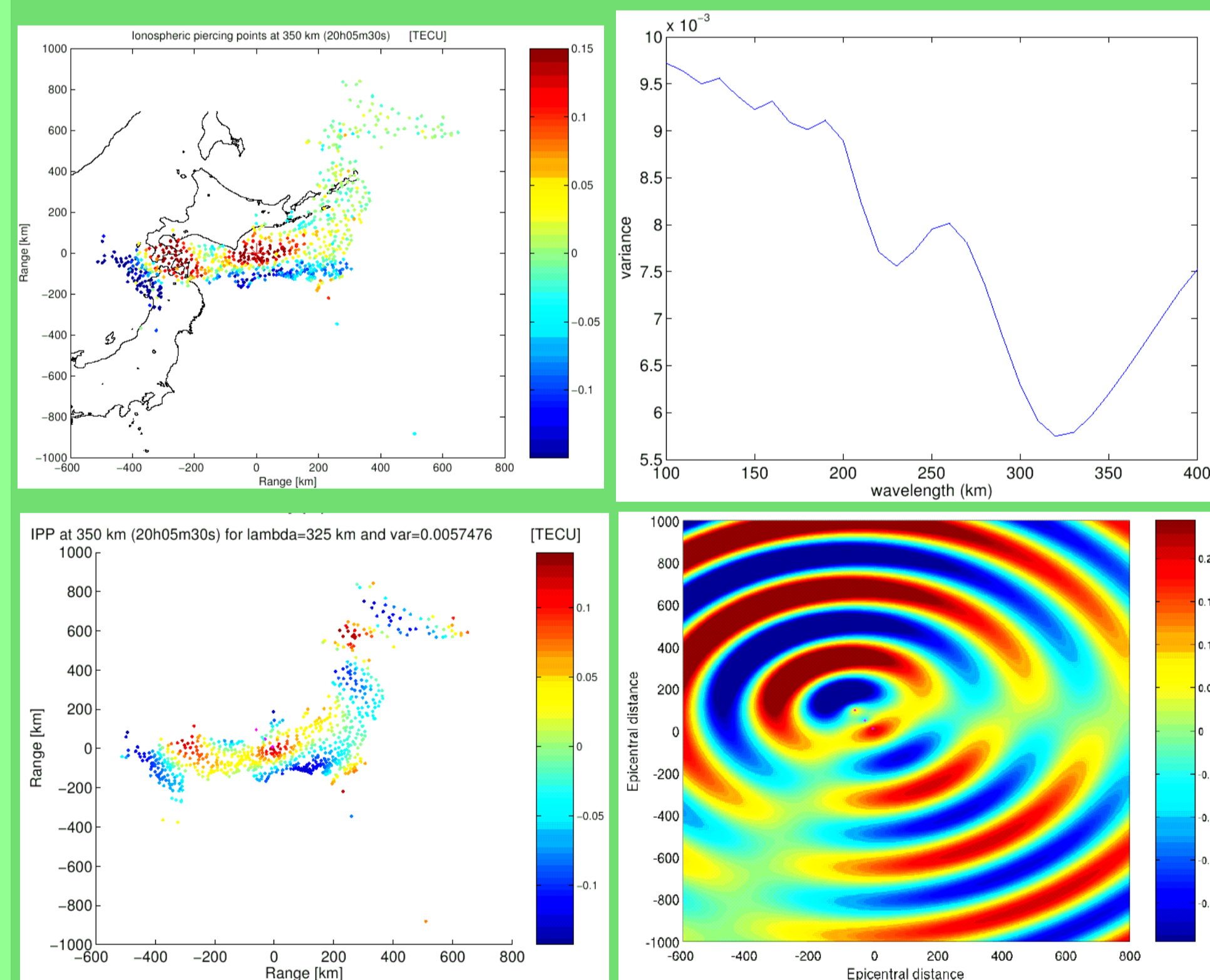


Fig. 4 : Preliminary result of the GPS data inversion tests. Top left : TEC data at ionospheric piercing points (IPPs). Top right : variance dependance with the wavelength. Bottom left : TEC values at IPPs calculated from inversion procedure. Bottom right : synthetic of the inversion result.

### Plasma coupling

Charged particles are reorganized under neutral wind effect. The dependencies in between are specified by the momentum equation (second hydrodynamic equation), written here under the assumption of Coulombian collisions only, for the three types of species that compose a partially ionized plasma : electrons, ions and neutral particles, after the formalism of [Schunk, R., Nagy, F., 2002].

$$\rho_i \frac{D\mathbf{v}_i}{Dt} = -\nabla \cdot \mathbf{p}_i + \rho_i \mathbf{g} + n_i q_i (\mathbf{E} + \mathbf{v}_i \times \mathbf{B}) - \rho_i \nu_{in} (\mathbf{v}_i - \mathbf{v}_n) - K n_e n_i (\mathbf{v}_i - \mathbf{v}_e)$$

$$\rho_e \frac{D\mathbf{v}_e}{Dt} = -\nabla \cdot \mathbf{p}_e + \rho_e \mathbf{g} + n_e q_e (\mathbf{E} + \mathbf{v}_e \times \mathbf{B}) - \rho_e \nu_{en} (\mathbf{v}_e - \mathbf{v}_n) - K n_e n_i (\mathbf{v}_e - \mathbf{v}_i)$$

$$\rho_n \frac{D\mathbf{v}_n}{Dt} = -\nabla \cdot \mathbf{p}_n + \rho_n \mathbf{g} + \rho_e \nu_{en} (\mathbf{v}_e - \mathbf{v}_n) + \rho_i \nu_{in} (\mathbf{v}_i - \mathbf{v}_n)$$

Where D/Dt is the convective derivative and :

$m_\alpha$	particule $\alpha$ mass
$q_\alpha$	particule $\alpha$ charge
$n_\alpha$	particule $\alpha$ numerical density
$\rho_\alpha$	mass density ( $\rho_\alpha = m_\alpha n_\alpha$ )
$\mathbf{v}_\alpha$	gaz $\alpha$ mean speed
$T_\alpha$	gaz $\alpha$ temperature
$p_\alpha$	partial pressure of gaz $\alpha$ ( $p_\alpha = n_\alpha k T_\alpha$ )
$\nu_{in}$	ion-neutral collision frequency
$\nu_{en}$	electron-neutral collision frequency
$K$	electron-ion collision ratio

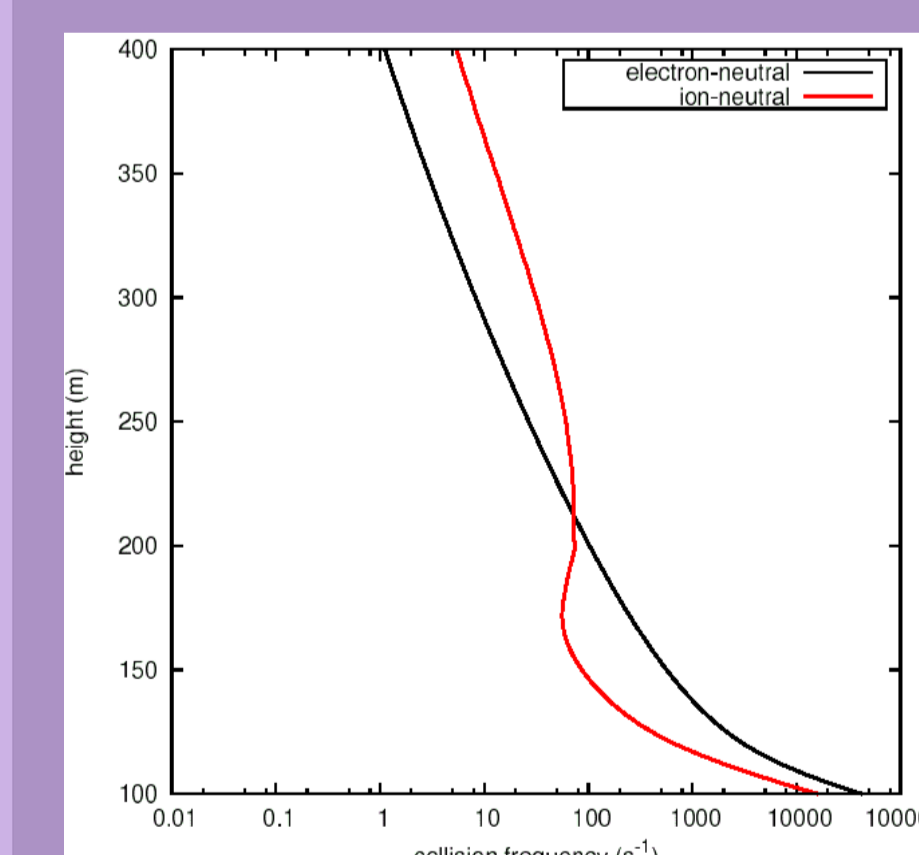


Fig.7 Collision frequency profiles

The continuity equation (first hydrodynamic equation) and the Maxwell equations are also considered. The energy equation (third hydrodynamic equation) is neglected in first approximation.

Fig.7 gives an exemple of two key parameters involved in transport equations : collision frequencies describe interaction between charged particles and neutral particles.

### Conclusions and perspectives:

Basic inversion here supplies a first fit of experimental data. Current developments are considering a more realistic modelling of source and atmospheric propagation of the synthesized acoustic waves. They will then account for dissipation and attenuation mechanisms involving parameters such as viscosity, aiming to constrain more completely the parameters of the rupture process by a final inversion.

#### Références :

- Yagi, Y., 2004. Source rupture process of the 2003 Tokachi-Oki earthquake determined by joint inversion of teleseismic body wave and strong ground motion data. Earth, Planets, and Space, 56, 311–316.
- Crespon, F., 2007. Tomographie 2D et 3D de l'ionosphère par GPS : applications aux aléas géophysiques. Thèse de doctorat, Institut de Physique du Globe de Paris.
- Schunk, R., Nagy, F., 2002. Ionospheres - Physics, Plasma Physics, and Chemistry. Cambridge Atmospheric and Space Science Series, Cambridge University Press.